

Failure Mechanisms of the Lotus Pond Landslide: A Reactivated Landslide from Large-Scale Cataclinal Slope Failure in the Three Gorges Reservoir Area of China

Zhen Feng, Nan Zhang, Hui Yan, and Zhenwei Dai

Abstract

The Lotus Pond landslide developed in a large-scale cataclinal slope on the right bank of Yangtze River. It has been reactivated by impounding of the Three Gorges Reservoir. Based on geological survey and experimental tests, deformation characteristics and failure mechanism have been ascertained. The Lotus Pond landslide is a successive landslide formed by three periods of sliding at different elevations; the three slides have similar shapes in the longitudinal profile. The toes of the later slides thrust and overlie the heads of the early slides on circular rupture surfaces. However, the successive slides exhibit different failure mechanisms, namely, buckling, planar slide, and “toe-break” mechanisms.

Keywords

Successive landslide • Buckling failure • Planar slide • Toe-break mechanism

1 Introduction

The water level of Yangtze River rose from approximately 90 to 145–175 m under the influence of the impounding of the three Gorges reservoir. More than 3000 landslides have been triggered by the impounding of water and fluctuation of the water level, including the Lotus Pond landslide (Yin et al. 2016). The Lotus Pond landslide is located on the south bank of Yangtze River in An’ping, Chongqing. The site is approximately 177 km away from the Three Gorges Dam. It was earlier a relocation site for An’ping town. According to the previous survey reports, the Lotus Pond landslide occurred thousands of years ago. In recent years, however, signs of reactivation of the landslide were observed. For example, a large number of cracks appeared in the ground, causing cracks in the walls of houses and other damage (Dai et al. 2015). This paper introduces the geological conditions and characteristics of the Lotus Pond landslide, and then reveals the failure mechanism that involves multiple periods and modes of slides.

2 Geological Background

The rock bedding in the Lotus Pond landslide dips to the north–east. The slope angle reaches up to 38° at the upper part and decreases to 12° at the lower part, where the main area of An’ping town and the constructions are located. The Lotus pond landslide originates from the south–eastern limb of the Guling Syncline, and the landslide is surrounded by folded mountains.

The outcrops around landslide area mainly include the overlying gravel soil of Quaternary Holocene eluvium, depleted landslide accumulations, and the underlying early Jurassic and late Triassic sandstone. The depleted landslide accumulations are composed of partially disturbed sandstone rock mass and basically preserve bedding planes and joints. The bedrock consists of sandstone layers of intermediate to

Z. Feng (✉)

Key Laboratory of Neotectonics and Geological Hazards,
Ministry of Land and Resources of PRC, Beijing, China
e-mail: fengzhenggs@126.com

Z. Feng

Institute of Geomechanics, Chinese Academy of Geological
Sciences, Beijing, China

N. Zhang

China Institute for Geo-Environment Monitoring, Geological
Survey, Beijing, China

H. Yan

Geological Survey Team 107, Chongqing Bureau of Geology and
Minerals Exploration, Chongqing, China

Z. Dai

Wuhan Center of China Geological Survey, Wuhan, China

high thickness and intercalated carbonaceous mudstone layers. The rock mass dips in the direction 320° – 350° with dip angles of 20° – 28° . Two conjugate sets of joints have developed in the rock mass. The attitude of one joint is 120° – 150° \angle 55° – 75° with a spacing of 1.1–2.0 m and that of the other joint is 40° – 70° \angle 60° – 85° with a spacing of 1.2–3.3 m.

Pore water is poorly stored within the superficial eluvium and the sliding mass. It is recharged mainly by the infiltration of natural precipitation, and it is discharged as springs and steams at the turning points of the terrace. The underground water table is deep within the depleted mass. In the upper area, the water table is located around the slide plane and is maintained relatively stable despite rainfall and reservoir water fluctuation. On the other hand, at the foot of the slides, the underground water table varies with the reservoir water level.

3 Geological Characteristics

The volume of the Lotus Pond landslide is about 90 million m^3 . The head of the Lotus Pond landslide is approximately 580 m wide, and its toe is approximately 1.1 km wide and is submerged in the Yangtze River (Fig. 1). The elevations of the landslide top at the head and landslide tip at the toe are 705 and 95 m, respectively. The total longitudinal slope length of the displaced mass is approximately 1800 m.

In the longitudinal profile, the ground surface appears as a broken line that can be divided into three sections according to the topography (Fig. 2). Geological surveys revealed that the three sections correspond to three periods of sliding events.

The lower and middle slides have a common slip plane and the upper slide occurs on a deeper weak plane. The slides present a spoon shape in profile that rock mass bedding and rupture surfaces are approximately parallel to the bedrock at the head, and then become sub-horizontal and even reverse to the slope surface at the foot.

The elevation of the head of the lower slide is 300–370 m. The depleted mass is very blocky, but the bedding planes and joints are still preserved. The thickness of the lower slide increases downslope from 50 to 120 m. The elevation of the middle slide ranges from 300 to 530 m. The geological structure and geometric form are similar to the lower slide. The foot is thrust and overlies on the head of the lower slide. The depth of the displaced mass varies from 30 m at the head to 60 m at the foot. Observation of drills and adits revealed that the slip plane is 0.3–0.5 m thick and is constituted of black carbonaceous claystone, generally angular clasts, and rock fragments. It contains approximately

60–80% silt and clay particles. Hence, the slip plane exhibits strong plasticity. Sand clasts and rock fragments were strongly sheared to a size of 0.5–6 cm and arranged directionally. The presence of slickensides and the steeped appearance indicate a landslide direction of 330° – 345° , which is in agreement with bedrock bedding direction.

The elevation of the upper slide is 400–705 m. The surface of rupture gradually turns into a circular arc at the foot, and it dips into the slope at an angle of 5° – 15° in the toe area. The depth of the depleted mass is approximately 15–30 m. The slip plane is 0.2 m thick on an average, and it is composed of 38–73% silt and clay and also exhibits high plasticity.

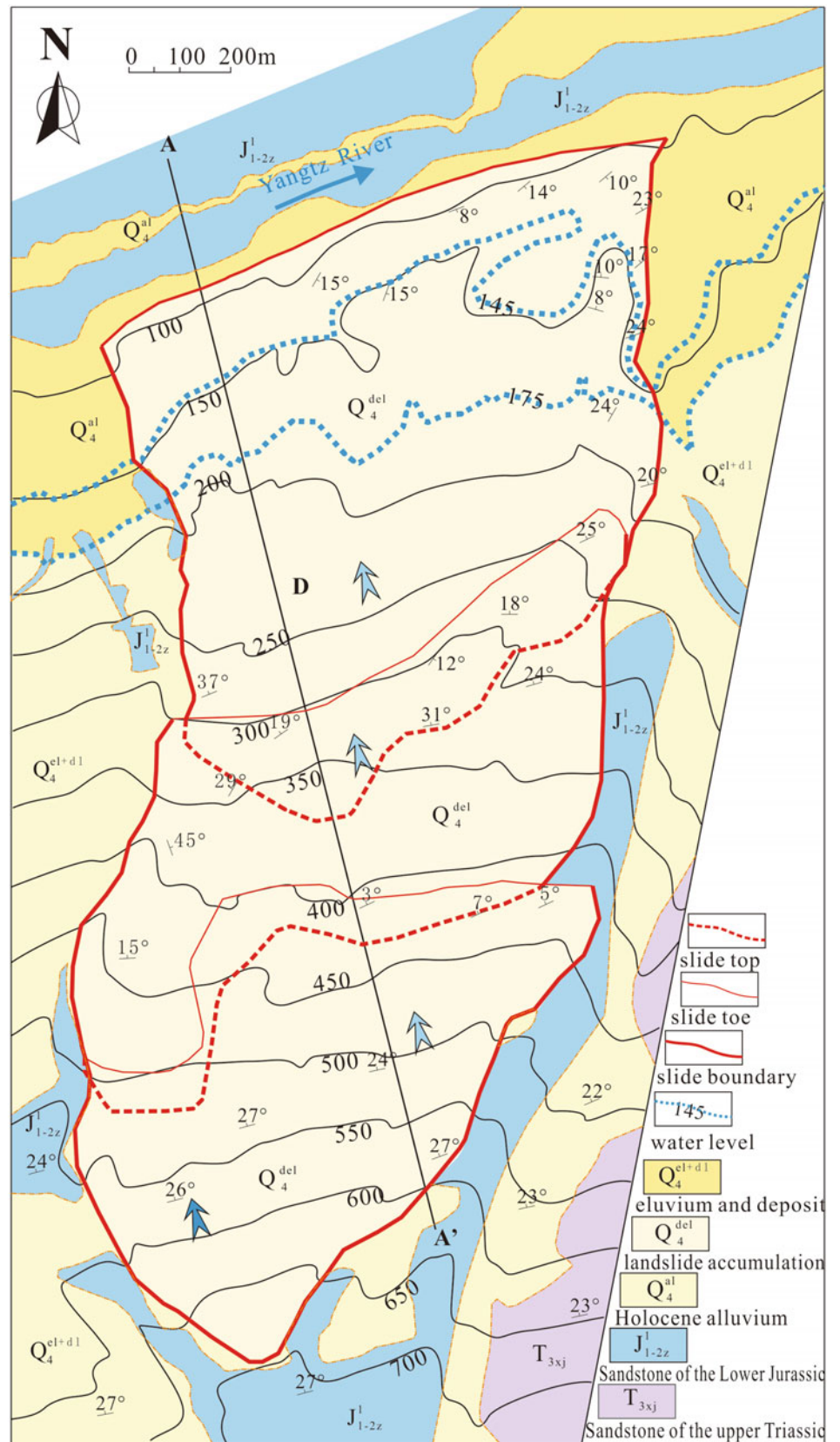
The western boundary of the Lotus pond landslide is formed by a north–east-striking ridge (Fig. 1). This ridge obstructs landslide movement in the dip direction. Field investigations revealed that the strata at the ridge is twisted slightly and dips to the north and north–east, while beyond the ridge, the dip direction of the strata is maintained between 330° and 345° . This variation is attributed to the thrust originating from the Lotus Pond landslide. Planar rotation occurred after the initial planar dip slide. Its case is similar to that of the Lianziya perilous rock mass (Yin 1995). The depleted mass slid north–west in the apparent dip direction owing to the obstruction in the west.

4 Failure Mechanism and Evolution

The Lotus Pond Landslide was formed by a sequence of three sliding events. ESR dating tests validated that the slip planes of the lower slide, middle slide, and upper slide formed approximately 120–130, 48–68, and 47–51 ka ago, respectively. The three slides clearly involve planar sliding. However, note that the bedrock beneath the rupture surface of the middle slide and upper slide have been barely disturbed, while that at the toe area of the lower slide rock mass is characterized by drag folding strata. It can be inferred that the lower slide underwent buckling failure.

Buckling develops in dip slope of relatively thin-layered strata with no sub-horizontal or gently inclined planes daylighting at the toe. The friction angle of the weak planes should be less than the dip angle so that the overlying rock mass can slip downslope, causing bending deformation. Most assessment methods for buckling failure in dip slope are based on the limit equilibrium technique in combination with Euler's buckling theory (Cavers 1981; Zhang et al. 1994). Using deflection formulas derived from the Euler–Bernoulli beam equation (Roark et al. 2002), a simplified solution can be obtained to calculate the length of the passive segment as follows (Garzon 2016):

Fig. 1 Geological map of the Lotus Pond landslide



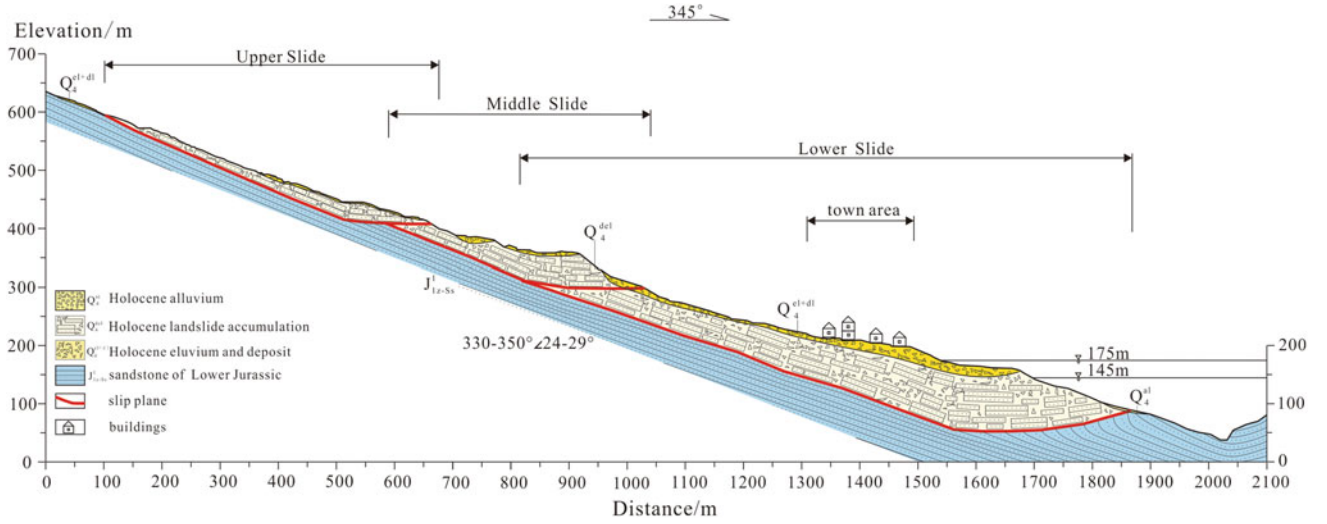


Fig. 2 Longitudinal profile of the Lotus pond landslide along A – A'

$$l = \sqrt{C_1^2 + 2C_1L_s} - C_1 \quad (1)$$

$$C_1 = 2.4(\gamma d \sin \alpha - c - \gamma d \cos \alpha \tan \varphi) / \gamma \cos \alpha \quad (2)$$

For slope under buckling failure, the potential; unit weight, γ ; slab thickness, d ; friction angle of slip plane, φ ; cohesion of the failure surface, c ; slope angle, α ; and total slope length, L_s , could be obtained to calculate the length of the passive segment l (Sergio 2016). In fact, the depleted range is usually less than the total slope length. Therefore, assessing the slope stability using total slope length is irrational.

For most landslides, determining the total slope length is difficult because of the lack of a significant boundary between the drive segment and passive segment after a large-scale displacement. In addition, the lower part of the passive segment underlies the landslide foot. For simplicity, the length of the surface of rupture, l_r , can be considered as the sum of the upper half of the passive segment, $l/2$, and the drive segment. Equation (1) is thus rewritten as Eq. (2).

$$l = \left(\sqrt{C_1^2 + 8C_1L_r} - C_1 \right) / 2 \quad (3)$$

Table 1 summarizes the dimensions and properties of the lower slide. Values of the physical and mechanical properties, such as the unit weight were obtained via experimental

tests. The slab thickness was determined by using drills located at the foot of the landslide. The lengths of the passive segment and drive segment were calculated as 262 and 966 m, respectively. The ratio of slab thickness to total slope length was 0.073.

The depleted range of the lower slide is shorter than the original slope which is approximately 1600 m. A steep scarp was formed after the lower slide occurred around 120–130 ka ago, and it provided a free face for initiating the middle slide. The middle slide occurred approximately 48–68 ka ago, and it proceeded via planar slide on the same slip plane as that of the lower slide. A simple sliding block model can be used for the stability analysis of the planar slide. The factor of safety (FOS) is described as the ratio of resistance to the drive force (Eq. 4). The FOS of planar slide for the lower slide is 0.63, which ensured sufficient drive force leading to the bending and buckling deformation of the passive segment.

$$K = (\gamma d \cos \alpha \cdot \tan \varphi + c) / \gamma d \sin \alpha \quad (4)$$

The middle slide was displaced by more than 200 m so that the foot thrusts and overlies the head of the early slide. The underlying bedrocks were exposed in the upper area of the slope. In contrast to the lower slide, the upper slide underwent a toe-break mechanism instead of buckling failure. The slip plane was buried approximately 30 m deep and

Table 1 Calculation parameters for the passive segment of the lower slide

Unit weight γ (kN/m ³)	Friction angle of slip plane φ (°)	Cohesion of the failure surface c	Slope angle, α (°)	Slab thickness d (m)	Length of the surface rupture l_r (m)	Length of the passive segment l (m)
27	37	22.4	15.2	90	1100	269

no joints are daylighted at the toe. The slide underwent cross-layer shear failure right behind the top of the Middle Slide. The stability mainly depends on the strength of the rock mass. The stability number can be used to assess slope stability (Hungr and Evans 2004).

$$N = (\gamma d \sin \alpha - \gamma d \cos \alpha \tan \varphi - c) / \sigma_c \quad (5)$$

where σ_c is the uniaxial compressive strength (UCS) of the rock mass. Three parameters, namely, the UCS of the intact rock, disturbance factor, and geological strength index are needed to derive the UCS using the Hoek–Brown failure criterion (Hoek et al. 2002).

5 Conclusion

The Lotus Pond landslide is a reactivated mega rockslide. It originated from a large-scale dip slope with gently inclined rock mass with joints. The displaced materials are mainly composed of fractured sandstone, which maintains partially disturbed structure. The Lotus Pond landslide is controlled by two layers of carbonaceous claystone that evolved into slip planes. In plan view, the apparent dip slide in the northeastern direction is involved because of the obstruction of the ridge in the west.

The Lotus Pond landslide is also known as a successive landslide that was formed during three periods of slides at different elevations. Though the depleted mass of three slides basically preserve the original structures and have similar shapes in the longitudinal profile, the three slides exhibit different failure modes and mechanism. The main

body of the lower slide underwent planar sliding movements, and bending and buckling occurred at the toe. Only planar slide occurred in the case of the middle slide when the weak layer was exposed after the early slide. A toe-break mechanism in combination with planar sliding occurred in the upper slide.

References

- Cavers, D.S.: Simple methods to analyze buckling of rock slopes. *Rock Mech.* **14**(2), 87–104 (1981)
- Dai, Z.W., Yin, Y.P., Wei, Y.J., et al.: Characteristics, origin and formation mechanism of the Outang landslide in the three gorges reservoir area. *Hydrogol. Eng. Geol.* **42**(6), 145–153 (2015)
- Hungr, O., Evans, G.S.: The occurrence and classification of massive rock slope failure. *Felsbau* **22**(2), 1–11 (2004)
- Garzon, S.E.R.: Analytical solution for assessing continuum buckling in sedimentary rock slopes based on the tangent-modulus theory. *Int. J. Rock Mech. Min. Sci.* **90**, 53–61 (2016)
- Hoek, E., Carranza-Torres, C., Corkum, B.: Hoek-Brown failure criterion-2002 edition. In: *Proceedings of the North American Rock Mechanics Symposium and Tunneling Association of Canada Conference*, pp. 267–273. Toronto, 7–10 July 2002
- Roark, R.J., Young, W.C., Budynas, R.G.: *Roark's Formulas for Stress and Strain*. McGraw-Hill, New York (2002)
- Yin, Y.P.: Engineering geology design supporting system and reinforcement design for Lianziya Perilous rock mass. *Geology Press, Beijing* (1995)
- Yin, Y.P., Huang, B.L., Wang, W.P., et al.: Reservoir-induced landslides and risk control in three gorges project on Yangtze River, China. *J. Rock Mech. Geotech. Eng.* **8**(5), 577–595 (2016)
- Zhang, Z.Y., Wang, S.T., Wang, L.S.: *Analytical Principle of Engineering Geology*. Geology Press, Beijing (1994)